Science and Engineering on Cray Supercomputers

Proceedings of the
Fourth International Symposium
Minneapolis, Minnesota, October 1988

Organized by Cray Research, Inc.

A Cray Research, Inc. book
Minneapolis, Minnesota
1988

THREE-DIMENSIONAL COMPUTATION OF BLOOD FLOW IN THE HEART

Charles S. Peskin and David M. McQueen

Courant Institute of Mathematical Sciences, New York University, 251 Mercer Street, New York, NY 10012 USA

INTRODUCTION

This report describes our progress towards the development of a three-dimensional computer model of the heart. The components of that model are (1) a subroutine FLUID that solves the incompressible Navier-Stokes equations on a cubic lattice, (2) a subroutine FIBER that computes the elastic forces generated by a system of fibers under tension, (3) a general-purpose program HEART3D that calls FLUID and FIBER as well as certain interaction routines to solve the coupled equations of motion of a viscous incompressible fluid containing an immersed system of elastic or contractile fibers, and finally (4) a particular arrangement of fibers that models the detailed anatomy of the heart, its valves, and the nearby great vessels.

Future applications of the model will include computer experiments concerning the normal and pathological function of the heart, computer-assisted design and evaluation of prosthetic cardiac valves, and computer simulation of cardiac imaging techniques. (For specific examples of such applications, see our earlier work based on a two-dimensional model of the left heart and the mitral valve [1-7].)

Of the four model components described above, the first three are operational (and tested), and the fourth is under development at this writing. In this paper, we shall give a summary description (with references) of the first three components, and then we shall conclude with a report on the fourth component: the construction of the cardiac model itself.

SUBROUTINE FLUID

A detailed description of this routine appears in [8]. Subroutine FLUID solves the incompressible Navier-Stokes equations in a cubic box with periodic boundary conditions. Chorin's projection method [9,10] is used with a uniform, cubic computational lattice. The method involves solution of (periodic) tridiagonal systems on each column, row, and file of the lattice. This is followed by the solution of a discrete Poisson equation for the pressure, which is used to restore the incompressibility of the computed velocity field. In the Poisson-equation step, the Fourier-Toeplitz method is used [11]. This fast Poisson solver employs two-dimensional (fast) Fourier transforms on each horizontal lattice plane, solution of (periodic) tridiagonal systems on each column of the lattice, and (fast) inverse Fourier transforms on each horizontal plane.

Our implementation of the projection method in Subroutine FLUID allows for the option of out-of-core storage of all three-dimensional arrays on an SSD, in case the program is being run on a CRAY X-MP and the problem size is too large for the central memory to accommodate such arrays. The basic strategy under the out-of-core option is to organize the three-dimensional data into horizontal planes and to store in central memory only a few adjacent planes at a time. Asynchronous input/output is used to overlap i/o with computation. In a typical sweep through the lattice, the data associated with plane K+1 are read into central memory while the data of plane K are updated, possibly using (but not modifying) the data of plane K-1, which are simultaneously being written out to the SSD. The central-memory arrays are organized as circular buffers so that there is no unnecessary data movement within central memory during such sweeps through all lattice planes. When the above-described strategy is used, the central memory requirements of the method grow only as the square, and not as the cube, of the number of lattice points in each space direction.

It is obvious that the foregoing strategy is applicable to those parts of the algorithm in which operations are performed separately on the different planes (e.g., the horizontal tridiagonal systems or the two-dimensional Fourier transforms on horizontal planes). Note, however, that the same strategy also works for the vertical tridiagonal systems, provided that those tridiagonal systems are all solved "at once". This means that the inner loops run over the different tridiagonal systems while the outermost loop controls the actual algorithm for solution of the tridiagonal systems.

The last remark also explains how Subroutine FLUID is

vectorized. In general, every step of the algorithm can be decomposed into either N or N^2 instances of the same sequence of operations to be performed essentially in parallel on different data. This allows for easy vectorization by letting the inner loops run over the different instances of the computation in question while the outer loops control the computation itself. A good example of this occurs in the two-dimensional Fourier transform, which we compute by first taking the Fourier transform in x and then in y. While taking the N separate transforms in the x direction, we let the inner loops run over y, and vice versa. This is so simple that even a user can do it! There is no need to worry about vectorization of the individual instances of the FFT computation.

For a detailed performance report on Subroutine FLUID, see [8]. Here, we note some key statistics that were obtained on a CRAY X-MP/SSD configuration with only one processor in use and with the machine dedicated to a single user. In the case considered here, the computation is performed on a 128^3 lattice. In these circumstances, the computational machinery of Subroutine FLUID runs at an average rate of 116 Mflops/sec. The overhead associated with communication between the SSD and central memory reduces this to an effective computation rate of 77 Mflops/sec.

SUBROUTINE FIBER [12,13]

This routine solves for the fiber forces, which are functions of the positions of the fiber points. These functions are constructed by postulating that adjacent points along a fiber are connected by springs, the elastic parameters of which may be constant [12] or time-dependent [13].

To improve the numerical stability of the method, the fiber configuration that is used in the computation of the fiber forces is not the configuration that is given at the beginning of each time step, but rather a configuration that approximates the unknown fiber position at the end of the time step. The approximation takes into account the influence of the fiber forces themselves on the fiber configuration at the end of the time step. This leads to a nonlinear fixed-point problem on each fiber. These problems are solved by Newton's method. The linear systems that arise at each Newton iteration take the form of periodic block-tridiagonal systems, with 3×3 blocks.

Vectorization and the optional use of the SSD are much the same in Subroutine FIBER as in Subroutine FLUID, described above. A complication here, however, is that the fibers may contain different numbers of points. This is handled by partitioning the fibers into groups, where all fibers in a group

contain the same number of points. Within a group, all of the nonlinear fixed point problems are solved "at once", so that vectorization is achieved by letting the innermost loops run over the different fibers.

HEART3D: A GENERAL-PURPOSE FIBER-FLUID CODE [12,13]

The general-purpose program HEART3D solves the coupled equations of motion of a viscous, incompressible fluid containing an immersed system of elastic or contractile fibers. These equations may be stated as follows:

$$\rho \left(\frac{\partial \underset{\sim}{u}}{\partial t} + \underset{\sim}{u} \cdot \nabla \underset{\sim}{u}\right) = - \nabla p + \mu \nabla^2 \underset{\sim}{u} + \underset{\sim}{F} \tag{1}$$

$$\nabla \cdot \underset{\sim}{u} = 0 \tag{2}$$

$$\underset{\sim}{F}(\underset{\sim}{x},t) = \int \underset{\sim}{f}(q,r,s,t)\, \delta(\underset{\sim}{x} - \underset{\sim}{X}(q,r,s,t))\, dq\, dr\, ds \tag{3}$$

$$\begin{aligned} \frac{\partial \underset{\sim}{X}}{\partial t} &= \underset{\sim}{u}(\underset{\sim}{X}(q,r,s,t),t) \\ &= \int \underset{\sim}{u}(\underset{\sim}{x},t)\, \delta(\underset{\sim}{x} - \underset{\sim}{X}(q,r,s,t))\, d\underset{\sim}{x} \end{aligned} \tag{4}$$

$$\underset{\sim}{f} = \frac{\partial}{\partial s} (T\, \underset{\sim}{\tau}) \tag{5}$$

$$T = \sigma(|\partial \underset{\sim}{X}/\partial s|, q,r,s,t) \tag{6}$$

$$\underset{\sim}{\tau} = \frac{\partial \underset{\sim}{X}/\partial s}{|\partial \underset{\sim}{X}/\partial s|} \tag{7}$$

Equations (1)-(2) are the incompressible Navier-Stokes equations in Eulerian form: $\underset{\sim}{u}(\underset{\sim}{x},t)$ is the fluid velocity, $p(\underset{\sim}{x},t)$ is the fluid pressure, and $\underset{\sim}{F}(\underset{\sim}{x},t)$ is the density of the force applied to the fluid by the immersed system of elastic or contractile fibers. The constants ρ and μ are the fluid density and viscosity. Equations (1)-(2) are solved by Subroutine FLUID, described above.

Equations (5)-(7) are the equations that define the fiber force in terms of the fiber configuration. Here $\underset{\sim}{X}(q,r,s,t)$ is the fiber configuration as a function of the Lagrangian parameters q,r,s which are chosen in such a way that q,r = constant along a fiber. The parameter s measures arc length along a fiber in the unstressed configuration only. In general, $|\partial \underset{\sim}{X}/\partial s| - 1$ is the fiber strain. The function T(q,r,s,t) is the fiber tension (T dq dr = force transmitted by the bundle of fibers dq dr), and $\underset{\sim}{\tau}(q,r,s,t)$ is the unit tangent to the fibers. The function σ defines the generalized Hooke's law that relates

See Color Figures P. 535 for fig. 1 (a, b).

the fiber tension to the fiber strain. Finally, $\underset{\sim}{f}(q,r,s,t)\ dq\ dr\ ds$ is the force applied to the fluid by the fibers that lie in the region swept out by $dq\ dr\ ds$. Equations (5)-(7) are solved by subroutine FIBER, as described above.

Equations (3)-(4) are the interaction equations, i.e., they couple the Eulerian variables and the Lagrangian variables. Note that both of these equations may be expressed in terms of the Dirac δ-function which expresses the local character of the fiber-fluid interaction. In the computational method, Equation (3) leads to a recipe for spreading the fiber force out onto the nearby lattice points of the fluid computation, while Equation (4) leads to an interpolation formula for the fluid velocity and hence to a prescription for how the fiber points should be moved.

Vectorization and the optional use of the SSD are more complicated in the interaction routines than in FLUID and FIBER themselves. Fundamentally, this is because the communication pattern is not fixed and because each fiber may interact with many (or even all) of the planes of the computational lattice of the fluid computation. Algorithms that overcome these difficulties are discussed in [12].

For empirical evidence of convergence of the computational method implemented in HEART3D, see [12]. Here, we give some results from a computation involving a fiber-wound toroidal tube in which the fibers are contractile [13]. This computation was performed on the CRAY-2 at the Minnesota Supercomputer Center, so the central memory size was adequate, and the out-of-core option (described above) was not used. The tube is made up of two nearby layers of spiral fibers, the inner layer having the opposite pitch to that of the outer layer. A wave of contraction propagates around the tube and pumps the internal fluid in the direction of the wave by a process that is known as "peristaltic pumping".

Figures 1-2 (see also Color Figure 1) show a cross section of the tube at three selected time steps (#816, 1008 and 1200). In each figure, the upper row shows results for a weak contraction, while the lower row shows the corresponding results for a stronger contraction.

Figure 1 shows velocity vectors in the laboratory frame of reference. The weaker and stronger contractions look qualitatively the same in this figure, although the distortion of the tube and the magnitude of the flow are obviously greater in the case of the stronger contraction. Figure 2, however, reveals a qualitative difference between the two cases. This is done by looking at the results from a frame of reference that rotates with the wave. In this frame, the wave appears still, and the particle trajectories (streaklines) reveal that, in the

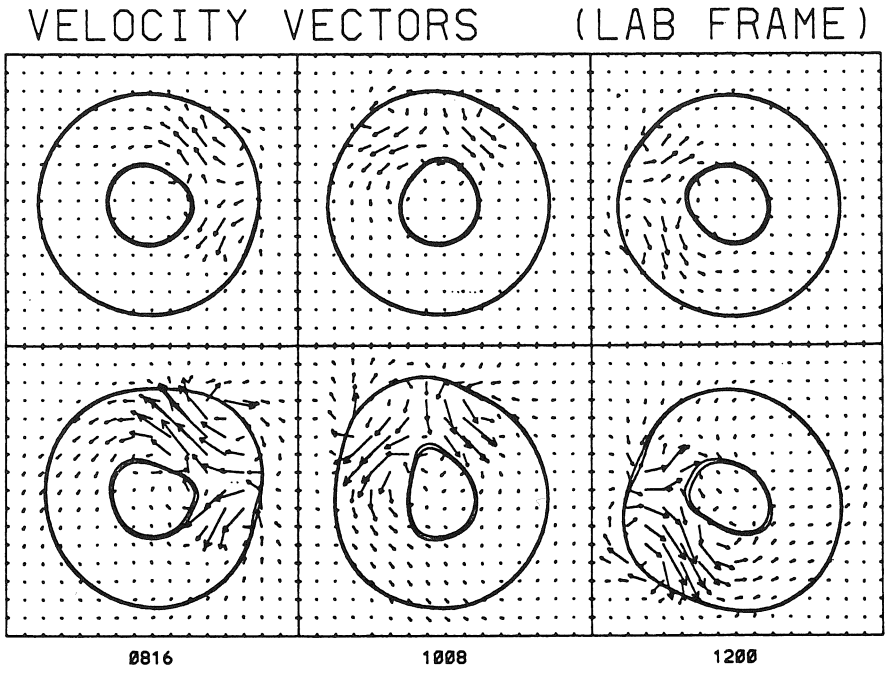

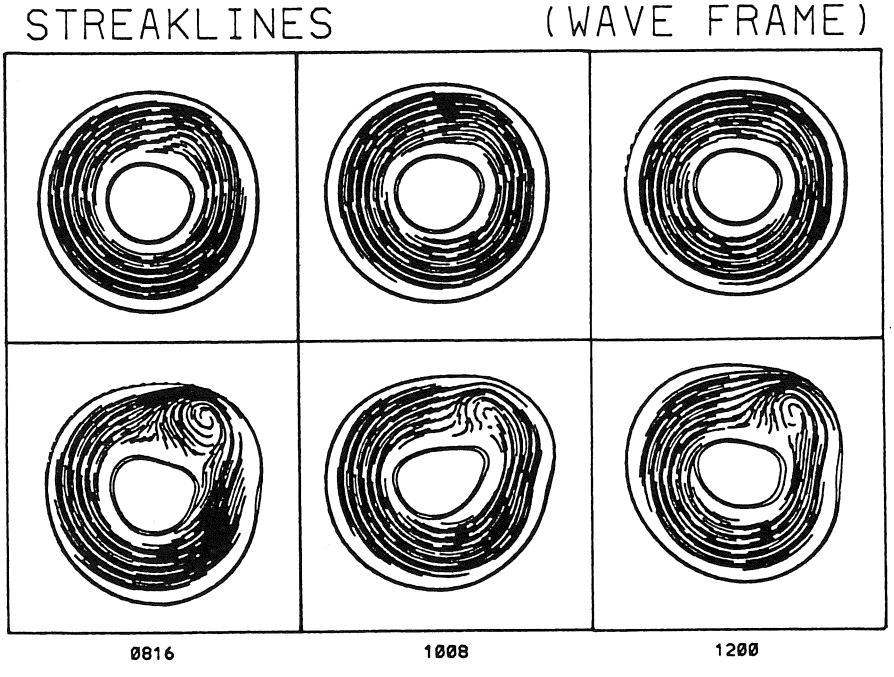

Figure 1 (TOP) and Figure 2 (BOTTOM)
PERISTALTIC PUMPING IN A CONTRACTILE TUBE

See Color Figures P. 536 for fig. 2 (a, b, c, d); P. 537 for fig. 2 (e, f, g, h).

case of the stronger contraction only, there is a small region of trapped, recirculating fluid that is convected along at the speed of the wave.

FIBER ARCHITECTURE OF THE HEART

HEART3D is a general-purpose code. To apply it to any particular problem, one must specify the (initial) arrangement in space of the fibers that interact with the fluid. In our case, this means that we must specify the anatomy of the heart in terms of its muscle fibers. (This is a much more difficult task than just specifying the location of the heart walls. Cross sections of the heart at different phases of the cardiac cycle are available from medical images, but such images do not reveal the directions in which the muscle fibers run.)

Fortunately, there have been a few empirical studies of the fiber architecture of the heart. Dissection techniques that make it possible to follow individual bundles of muscle fiber over great distances were developed by C. E. Thomas [14], who used these techniques to reveal the global fiber architecture of the right and left ventricles. Quantitative measurements of fiber angle in the left ventricle have been made by Streeter and his colleagues [15,16], who ultimately arrived at the generalization that the left ventricular fibers follow geodesic curves on a nested family of toroidal surfaces [16]. (For a theoretical study that accounts for this result, see Peskin [17].)

Our first three-dimensional model of the heart, now under construction, is primarily based on the qualitative observations of Thomas, although we also make use of Streeter's more detailed description of fiber architecture of the left-ventricular wall. The ventricular part of the model is complete and will be briefly described here. The valves, the atria, and the great vessels remain to be constructed.

The upper border of the model ventricles is a plane called the "base", which contains the four valve rings. Below the base and parallel to it is a plane called the "equator", in which the model ventricles achieve their greatest diameter. Below the equator, the model ventricles taper down to a point which is called the "apex" of the heart.

The part of the heart below the equator consists of several fiber layers in the form of generalized cones. Each such layer has two sheets. The layers have the following names and descriptions. (See Color Figure 2.)

Outer/inner layer This consists of two conical sheets, one inside the other. The sheets have a common apex at the apex of

the heart. The outer sheet surrounds the heart as a whole and the inner sheet forms the innermost lining of the left ventricle. The fibers are rays which make a transition from one sheet to the other at the apex.

Right-inner/left-outer layer This layer also consists of two conical sheets but side by side. The right sheet is the inner lining of the right ventricle and the left sheet is the outermost layer of the left ventricle except for the outer sheet of the outer/inner layer. The two sheets of the right-inner/left-outer layer have a common apex at the apex of the heart, and they coincide along the right face of the interventricular septum. The fibers are horizontal as they cross the midline of the septum. From there, they follow geodesic curves which eventually bring them up to the level of the equator.

Toroidal layers These layers make up the bulk of the left ventricular wall. The name "toroidal" comes from the work of Streeter et al. [16] in which the bulk of the left ventricle is described as a nested family of toroidal shells. (Thomas calls this whole structure "the cylinder of the left ventricle".) Following Streeter et al. [16], we model the part of each toroidal layer that lies below the equator as a double-sheeted truncated cone. The two sheets have a common axis (but not a common apex). They meet along a circle at which the fibers make a smooth transition from one sheet to the other. Away from this circle, the fibers spiral up to the equator following geodesic curves that become more nearly vertical as the fibers ascend.

In all of the layers that we have just described, the fibers eventually reach the equator. From there, the fibers must be continued somehow to reach the valve rings [14]. We do this in the following expedient way. Let the equatorial plane be denoted $z = 0$ and let the plane of the base be denoted $z = 1$. Suppose we have a layer whose cross section in the plane of the equator is $f_0(x,y) = 0$ and we want to continue this layer in such a way that its cross section in the plane of the base coincides with one or more of the valve rings which are collectively described by $f_1(x,y) = 0$ in the plane $z = 1$. For example, the layer in question may have an elliptical cross-section in the equatorial plane, $z = 0$:

$$f_0(x,y) = \alpha_0(x-x_0)^2 + \beta_0(x-x_0)(y-y_0) + \gamma_0(y-y_0)^2 - 1 \quad (8)$$

and it may join with a pair of elliptical valve rings in the plane of the base

$$f_1(x,y) = \prod_{j=1}^{2} [\alpha_j(x-x_j)^2 + \beta_j(x-x_j)\,(y-y_j) + \gamma_j(y-y_j)^2 - 1] \qquad (9)$$

Then the surface

$$0 = f(x,y,z) \equiv (1-z)\, f_0(x,y) + z\, f_1(x,y) \qquad (10)$$

has the required cross-sections in the planes $z = 0$ and $z = 1$ and is given by a simple analytic formula. (In the example considered here, the surface $f(x,y,z) = 0$ defines a tube with a bifurcation: the cross section is a single ellipse at $z = 0$ but a pair of ellipses at $z = 1$.) Once we have an analytic formula for the surface, it is not too difficult to solve (numerically) the differential equations for a geodesic on this surface and hence to continue the fibers up to the valve rings. This completes the construction of the ventricles.

SUMMARY AND CONCLUSIONS

We have developed a general-purpose program HEART3D which can be used to solve the coupled equations of motion of a viscous incompressible fluid and an immersed system of elastic or contractile fibers. We have applied this program to the problem of peristaltic pumping in a contractile, fiber-wound tube, and we have prepared for computations involving the heart by constructing a fiber-based model of the cardiac ventricles. When this model has been expanded to include the valves, the atria, and the great vessels, we shall be ready for computer experiments on cardiac fluid dynamics. It is our hope that such experiments will prove useful in the study of normal and pathological heart physiology and also in the design of prosthetic cardiac valves.

ACKNOWLEDGEMENTS

This work is primarily supported by the National Institutes of Health under research grant HL17859. Additional support has been derived from the National Science Foundation under DMS8701895, and additional computer time has been generously made available by the Minnesota Supercomputer Center (MSC). We are also indebted to the MSC for technical support including the preparation of a videotape that shows peristaltic pumping in the contractile toroidal tube. Hadil Sabbagh has made substantial contributions to our local three-dimensional graphics capability. The camera-ready copy for this paper was prepared by Connie Engle.

REFERENCES

1. Peskin CS (1977) Numerical analysis of blood flow in the heart. J Comput. Phys. 25:220-252

2. Peskin CS and McQueen DM (1980) Modeling prosthetic heart valves for numerical analyis of blood flow in the heart. J. Comput. Phys. 37:113-132

3. Peskin CS (1982) The fluid dynamics of heart valves: experimental, theoretical, and computational methods. Ann. Rev. Fluid Mech. 14:235-259

4. McQueen DM, Peskin CS, and Yellin EL (1982) Fluid dynamics of the mitral valve: physiological aspects of a mathematical model. Am. J. Physiol. 242:H1095-H1110

5. Meisner JS, McQueen DM, Ishida Y, Vetter HO, Bortolotti U, Strom JA, Frater RWM, Peskin CS, and Yellin EL (1985) Effects of timing of atrial systole on LV filling and mitral valve closure: computer and dog studies. Am. J. Physiol. 249: H604-H619, 1985

6. McQueen DM and Peskin CS (1983) Computer-assisted design of pivoting disc prosthetic mitral valves. J. Thorac. Cardiovasc. Surg. 86:126-135

7. McQueen DM and Peskin CS (1985) Computer-assisted design of butterfly bileaflet valves for the mitral position. Scand. J. Thor. Cardiovasc. Surg. 19:139-148

8. Greenberg S, McQueen DM, and Peskin CS (1987) Three-dimensional fluid dynamics in a two-dimensional amount of central memory. In: Wave Motion: Theory, Modeling, and Computation. Proceedings of a Conference in Honor of the 60th Birthday of Peter D. Lax. (A.J. Chorin, ed.) Springer-Verlag, New York, pp. 85-146.

9. Chorin AJ (1968) Numerical solution of the Navier-Stokes equations. Math. Comp. 22:745-762

10. Chorin AJ (1969) On the convergence of discrete approximations to the Navier-Stokes equations. Math. Comp. 23:341-353

11. Fischer D, Golub G, Hald O, Leiva C, and Widlund O (1974)

On Fourier-Toeplitz methods for separable elliptic problems. Math. Comp. 28:349-368

12. Peskin CS and McQueen DM (c.1988) A three-dimensional method for blood flow in the heart: I. Immersed elastic fibers in a viscous incompressible fluid. J. Comput. Phys., in press.

13. McQueen DM and Peskin CS (c.1988) A three-dimensional method for blood flow in the heart: II. Contractile fibers. J. Comput. Phys., submitted.

14. Thomas CE (1957) The muscular architecture of the ventricles of hog and dog hearts. Am. J. Anatomy 101:17-57

15. Streeter DD Jr, Spotnitz HM, Patel DP, Ross J Jr, and Sonnenblick EH (1969) Fiber orientation in the canine left ventricle during diastole and systole. Circ. Res. 24:339-347

16. Streeter DD Jr, Powers WE, Ross MA, and Torrent-Guasp F (1978) Three-dimensional fiber orientation in the mammalian left ventricular wall. In: Cardiovascular System Dynamics (J. Baan, A. Noordergraaf, and J. Raines, eds.) M.I.T. Press, Cambridge MA, pp. 73-84.

17. Peskin CS (c.1988) Fiber architecture of the left ventricular wall: an asymptotic analysis. Commun. Pure and Applied Math., in press.

TRADEMARKS

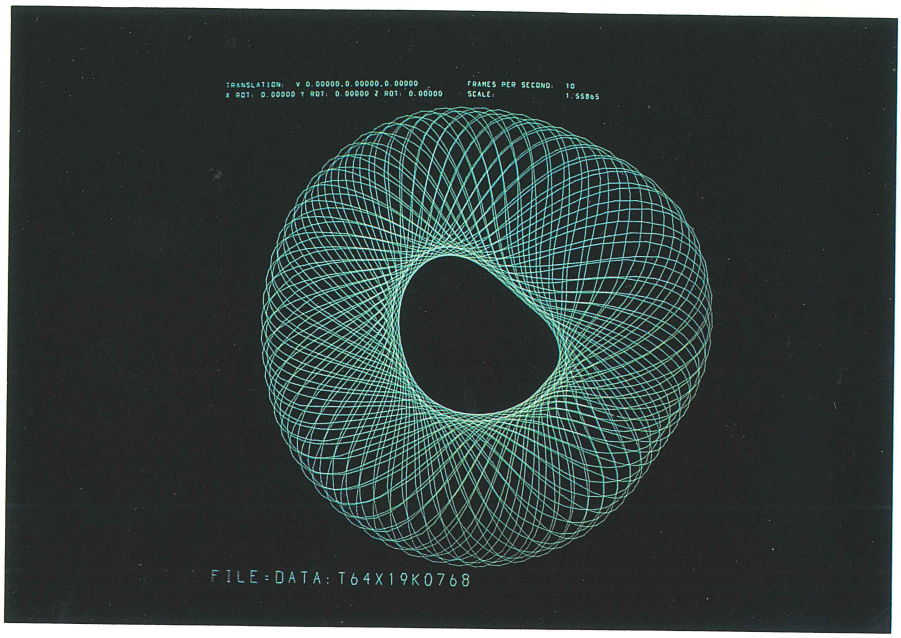

(a)

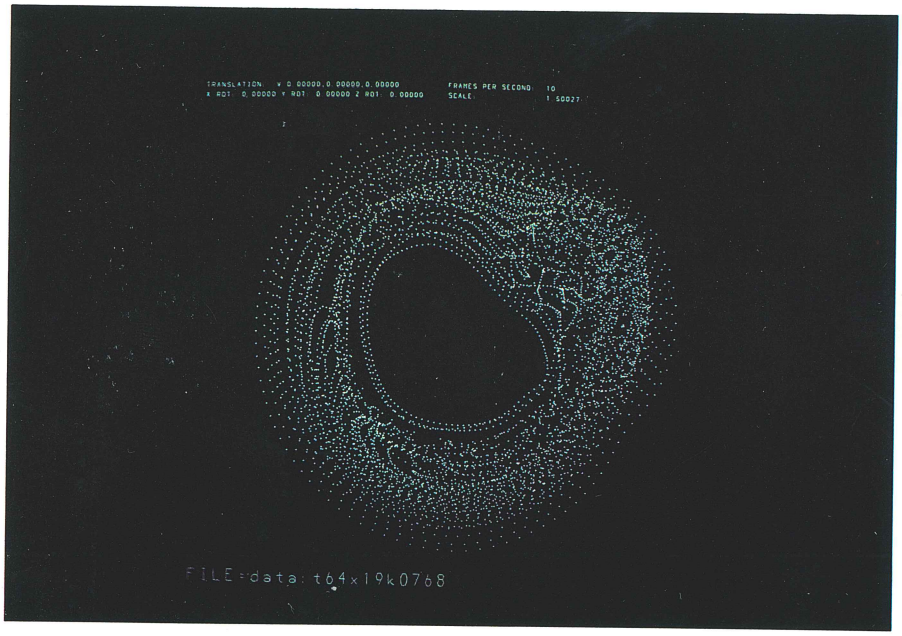

(b)

Figure 1 (a, b): *(from Charles S. Peskin and David M. McQueen, pg. 131)* (a) Two-layer fiber-wound contractile tube. (b) Fluid particles in the interior of the tube.

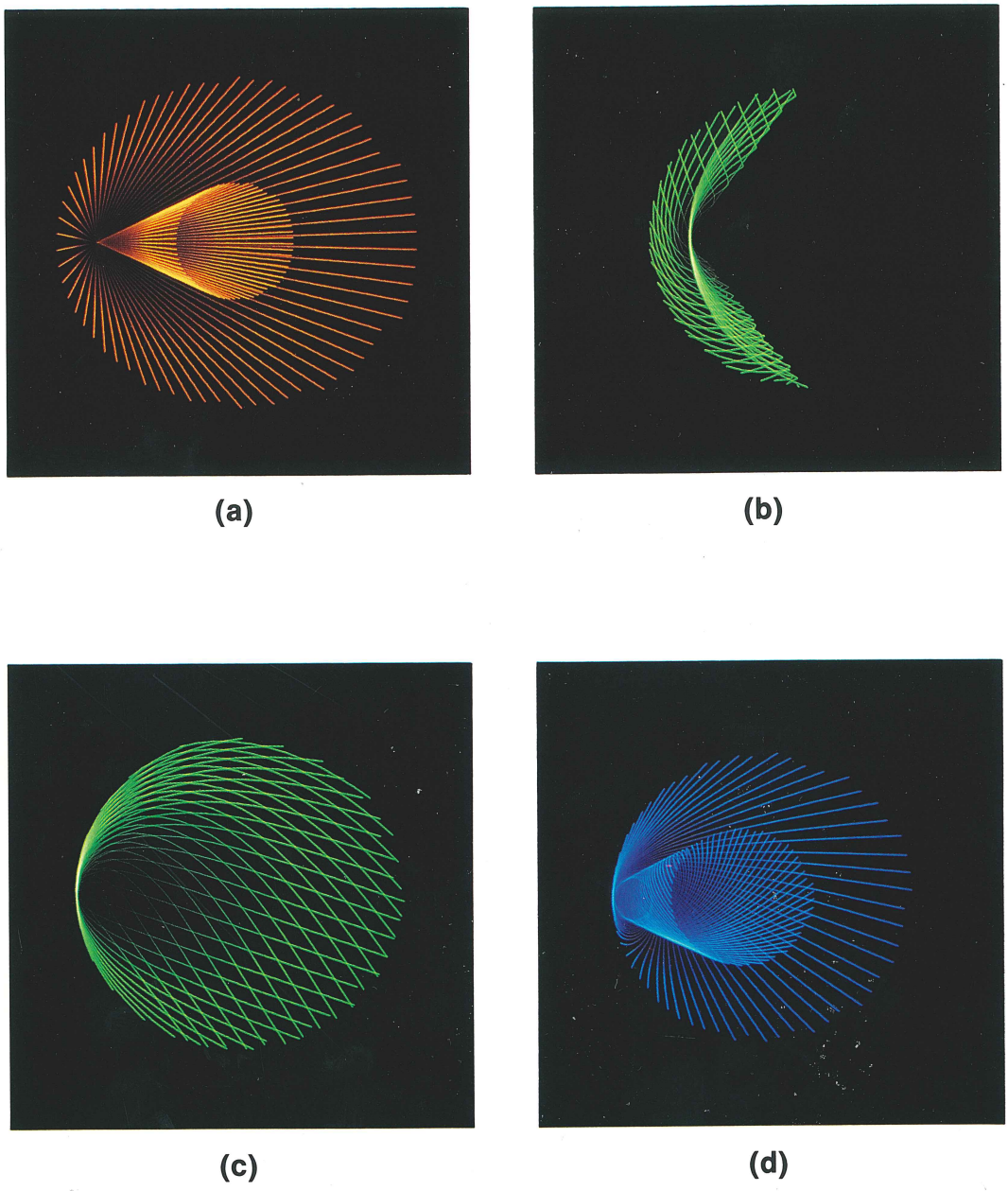

Figure 2 (a, b, c, d): *(from Charles S. Peskin and David M. McQueen, pg. 133)* Fiber model of the cardiac ventricles. (Only the part below the equator is shown. The view is looking down towards the apex.) (a) Outer/inner layer. (b) Right part of right-inner/left-outer layer. (c) Left part of right-inner/left-outer layer. (d) Largest of the toroidal layers.

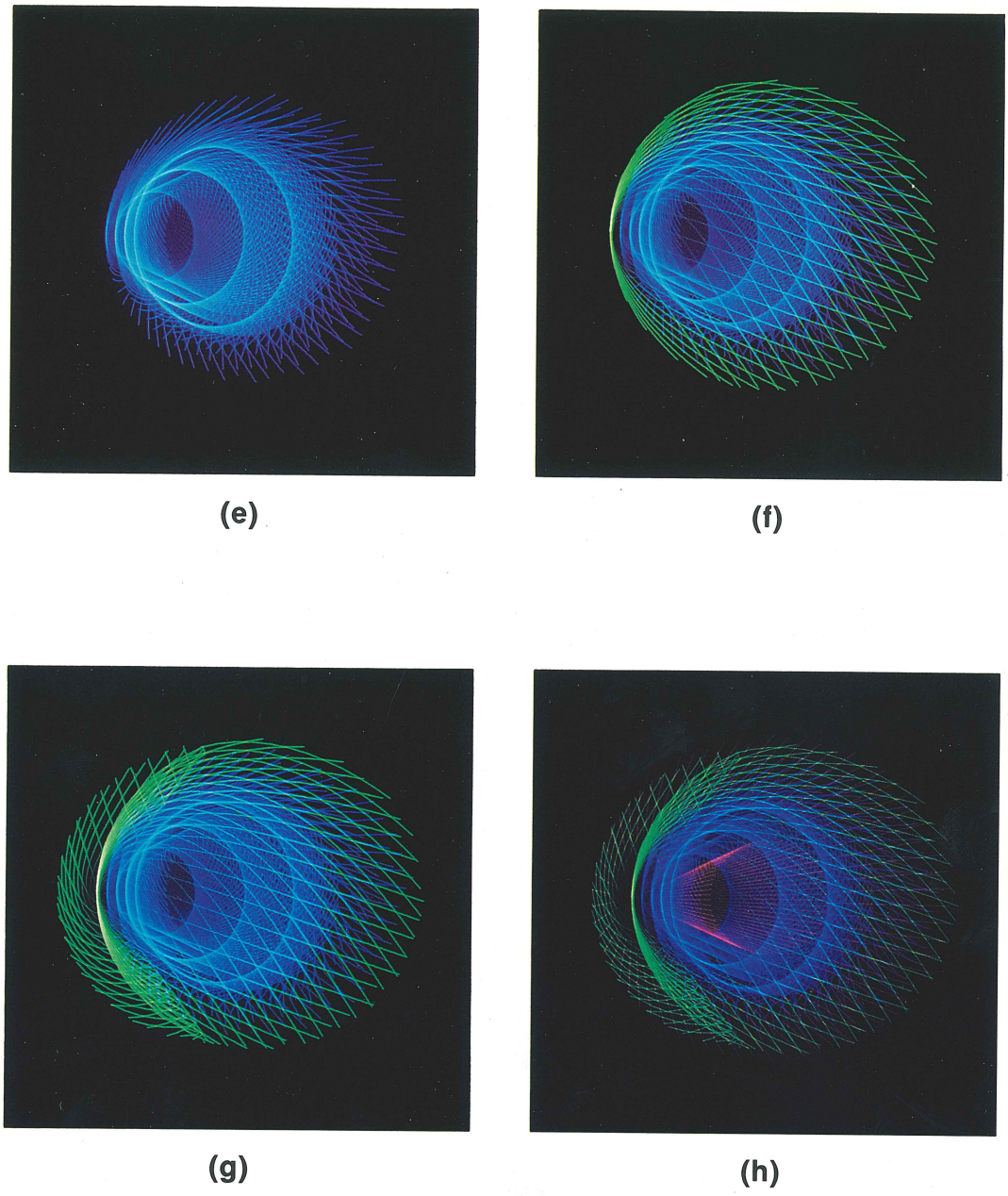

Figure 2 (e, f, g, h): *(from Charles S. Peskin and David M. McQueen, pg. 133)* (e) Nested toroidal layers. (f) Toroidal layers surrounded by left-outer layer. (g) Toroidal layers + right inner/left-outer layer (The crescent-shaped cavity is the right ventricle). (h) All layers shown together.